



Heat and cold wave intensity and spatial extent on the Iberian Peninsula: future climate projections (2050–2095)

Alejandro Díaz-Poso¹ · Nieves Lorenzo² · Alberto Martí¹ · Dominic Royé³

Received: 17 July 2024 / Accepted: 22 April 2025 / Published online: 9 May 2025
© The Author(s) 2025

Abstract

In the current context of global warming, heat waves are extreme climate events that have captured the focused attention of the scientific community due to their increasing impact on public health, energy consumption, fire risk, and agriculture/livestock. Although less studied, cold waves remain an extreme climate event to be reckoned with, with implications for transport systems, energy consumption, crops, and human health. This paper presents an analysis of the representative concentration pathway (RCP) 4.5 and RCP 8.5 scenarios under European Coordinated Regional Downscaling Experiment simulations using the excess heat factor (EHF) and excess cold factor indices for the Iberian Peninsula and the Balearic Islands (IPB). The study period is the second half of the 21st Century (2050–2095) with respect to the historical reference period (1971–2000), and the dimensions analysed are intensity and spatial extent. The projected EHF results show a very significant increase on these dimensions. The average change in maximum heat wave intensity for the IPB is projected to be 144%, which is 40% more than in the 2021–2050 period. The largest changes are expected in the east and southeast and will reach 300%. The average spatial extent of heat waves is projected to increase by 1–2.7% per decade, significantly amplifying fire risk, energy demand, and human exposure. For cold waves, both dimensions will decrease. The average change in maximum cold wave intensity will be –16%, and the maximum extent will decrease much more than the average, with decreases between –0.7%/decade and –3.2%/decade, which will imply lower exposure. Despite this, the RCP 8.5 scenario will record a higher maximum intensity of cold waves in the IPB than the RCP 4.5 scenario, demonstrating that such events will continue to exist in the second half of the century, even with high radiative forcing.

Keywords Climate change · ECF · EHF · Extreme temperatures · Future projections

1 Introduction

✉ Alejandro Díaz-Poso
a.diaz.poso@usc.es

Nieves Lorenzo
nlorenzo@uvigo.es

Alberto Martí
alberto.marti@usc.es

Dominic Royé
droye@mbg.csic.es

¹ Department of Geography, University of Santiago de Compostela, Praza da Universidade 1, 15782 Santiago de Compostela, Spain

² Environmental Physics Laboratory (EphysLab), CIM-UVIGO, University of Vigo, Edificio Campus da Auga, 32004 Ourense, Spain

³ Misión Biológica de Galicia (MBG) - CSIC, Avda. de Vigo, 15707 Santiago de Compostela, Spain

In the face of escalating global temperatures attributed to ongoing climate change, extreme climate events have become a focal point for scientific inquiry due to their profound implications for society and the natural environment (IPCC 2023). Among these extreme climate events, heat waves, unusual periods of excessive heat, have garnered a great deal of attention, and the scientific community has quantified concerning increases in intensity, duration, spatial extent, and frequency in recent decades (Kuglitsch et al. 2010; Acero et al. 2017; Perkins-Kirkpatrick and Lewis 2020; IPCC 2023; Oliveira et al. 2022; Serrano-Notívoli et al. 2022; Díaz-Poso et al. 2023a; Paredes-Fortuny and Khodayar 2023; Khodayar and Paredes-Fortuny 2024). Such extreme events have implied severe consequences for population health (Guo et al. 2017; Liss et al. 2017; Royé et al. 2020; Tobías et al. 2023a; Lüthi et al. 2023; Ballester et al.

2023). Cold waves, although less studied in recent decades, are still important extreme meteorological events (Wibig et al. 2009; Lhotka and Kyselý 2015; Spinoni et al. 2015; Piticar et al. 2018; Tomczyk et al. 2018; Smid et al. 2019; Bitencourt et al. 2019; Espín-Sánchez and Conesa-García 2021; Serrano-Notívoli et al. 2022). Despite global warming and declining cold-wave frequency in recent decades, cold-related mortality will not decline due to population aging (Chen 2024). Ambient cold exposure has multiple health effects (Gao et al. 2024) that may even exceed heat wave mortality (Vardoulakis et al. 2014; Gasparrini et al. 2015; Carmona et al. 2016).

Globally, each of the last four decades has been successively warmer than any previous decade since pre-industrial times (IPCC 2023), and the last nine years have been the warmest since records have been kept (Copernicus 2023a; Berkeley Earth 2024).

Before mid-century, global temperatures will reach 1.5 °C above pre-industrial levels (IPCC 2023). In fact, 2023 was 1.48 °C warmer than pre-industrial levels, making it the warmest year on record (Copernicus 2023a). Extreme heat waves have gone from occurring once every 50 years in the pre-industrial period to once per decade currently (IPCC 2023), and under warming levels above 1.5 °C, return periods will continue to decrease (Lüthi et al. 2023). The current anthropogenic radiative forcing, 2.72 W/m² (IPCC 2023), is expected to generate a temperature increase trajectory at the end of the century, 2081–2100, more than 1.8 °C above pre-industrial levels, far exceeding the forecast associated with the representative concentration pathway (RCP) 2.6 scenario.

The European continent has experienced an average warming in the last five years that is almost double that of the planet as a whole (2.2 °C above pre-industrial levels) and that has been faster, both in winter and summer, than that of any other continent (Copernicus 2023b). Europe is therefore becoming a leading climate hotspot (Van Daalen et al. 2022). In parallel, cold waves in the northern mid-latitudes have experienced a decrease in their spatial extent and a warming rate 3–5 times higher than the rate of increase of global mean temperature in 1990–2018 (Van Oldenborgh et al. 2019).

This does not mean that extremely cold temperature events will cease to occur. Although less frequent, especially in Scandinavia and northeastern Russia (Carvalho et al. 2021), cold waves will continue to occur in Europe throughout this century (Kodra et al. 2011). An example of this was the recent cold wave in Fennoscandia in 2024 (Pinto et al. 2024).

The Mediterranean region stands out most for its warming (Giorgi 2006; Fischer and Schär 2009; Jacob et al. 2014; Vicedo-Cabera et al. 2018; Zittis et al. 2019; Vogel et al. 2020; Cos et al. 2022; Feng et al. 2022; Oliveira et al. 2022,

Urdiales-Flores et al. 2023), which is expected to exceed global rates by 20% (50% in summer) during this century (Lionello and Scarascia 2018), further accentuating its already known vulnerability (Diffenbaugh et al. 2007; Bacchin et al. 2008; D’Ippoliti et al. 2010; Kendrovski et al. 2017; Spinoni et al. 2018; MedECC 2020).

Already, one in three heat-related deaths is estimated to be related to anthropogenic climate change (Vicedo-Cabrera et al. 2021). Alongside Italy and Greece, Spain and Portugal are, according to recent estimates, the countries with the highest heat-related mortality rates and the most excess deaths (Mayrhuber et al. 2018; Ballester et al. 2023; Barriopedro et al. 2023). In addition, with the Scandinavian countries, they also have the highest rate of excess winter mortality and the lowest level of domestic thermal efficiency in Europe (Healy 2003; Ordanovich et al. 2023). Future cold waves, although less severe, could have a greater impact on health because their lower frequency could lead to a decrease in risk perception and adaptive measures (Pinto et al. 2024). Consequently, increased temperatures will pose an even greater health threat in the spatial context of the Iberian Peninsula and Balearic Islands (IPB) (Fig. 1).

Future projections for the IPB show a clear consensus on the increase in intensity, frequency, duration, and spatial extent of heat waves (Fischer and Schär 2010; Pereira et al. 2017; Viceto et al. 2019; Molina et al. 2020; Lorenzo et al. 2021; Lorenzo and Alvarez 2022) whereas these dimensions will decrease for cold waves, especially frequency and spatial extent (Ramos et al. 2011; Pereira et al. 2017; Viceto et al. 2019; Serrano-Notívoli et al. 2022; Díaz-Poso et al. 2023b). Therefore, the current increase in population exposure to extreme heat (Pascaline and Rowena 2018) highlights the need for timely implementation of robust adaptation measures to reduce heat-related mortality (Gosling et al. 2017), such as climate shelters or early warning systems for heat-related health risks (Serrano-Notívoli et al. 2023; Tobías et al. 2023b) because existing ones have proven to be insufficient (Ballester et al. 2023; Domeisen et al. 2023).

Although recent studies have contributed to substantially improving our understanding, there is still no universally accepted quantitative definition of a heat/cold wave (Perkins and Alexander 2013; Perkins 2015; Añel et al. 2017; Barriopedro et al. 2023). The vast majority of indices and organizations use maximum/minimum temperature thresholds, as well as minimum extent and duration (García-Herrera et al. 2010; Perkins and Alexander 2013; Perkins 2015; Russo et al. 2015; Spinoni et al. 2015; Acero et al. 2017; Pereira et al. 2017; Lavaysse et al. 2019; Smid et al. 2019; Viceto et al. 2019). Because there are no optimal thresholds for a universal definition to be generalized, this is probably an infeasible goal (Barriopedro et al. 2023).

Both heat and cold waves can be characterized by considering four dimensions: intensity, duration, frequency, and

Fig. 1 Study area showing the limits of the Iberian Peninsula and Balearic Islands and terrain elevation



spatial extent (Raei et al. 2018). The dimensions of intensity and spatial extent have been studied little in the spatial domain of the IPB (Sánchez-Benítez et al. 2020; Espín-Sánchez and Conesa-García 2021; Lorenzo et al. 2021; Serrano-Notívoli et al. 2022; Díaz-Poso et al. 2023a, b).

Developed by Nairn and Fawcett (2013), the excess heat factor (EHF) is a biometeorological index that integrates the dimension of intensity and the acclimatization process of the human body (Xu et al. 2016) and has been shown to be effective in predicting health risks associated with extreme heat events (Scalley et al. 2015; Nairn et al. 2018; Williams et al. 2018; Sheridan et al. 2021; Wondmagegn et al. 2021). It has also been tested in the specific spatial context of the IPB (Morais et al. 2020; Royé et al. 2020; Oliveira et al. 2022), where it has proved to be faster than other indices in detecting heat wave conditions (Díaz-Poso et al. 2023a). This greater sensitivity to local temperature variations than other indices that use maximum/minimum temperature thresholds (Nairn et al. 2018) makes it possible to alert the population earlier to an extreme event, which is a key factor in minimizing health impacts. This index also has its conceptually analogous version, the excess cold factor (ECF) (Nairn and Fawcett 2013). Because their values are relative to the local climate, these biometeorological indices can be used in any location for which data are available. Climate projections that have used the EHF/ECF indices in the IPB domain for the near future (2021–2050) confirm an average increase (decrease) of 65% (−23.3%) in the maximum intensity of heat (cold) waves and 6–8% (−2.4%; −5.5%)

per decade in their maximum spatial extent (Lorenzo et al. 2021; Díaz-Poso et al. 2023b).

The objective of this work is to continue to advance our knowledge of the evolving intensity and spatial extent of heat and cold waves in the IPB in the second half of this century (2050–2095), using the EHF/ECF indices based on five simulations of the EURO-CORDEX project for the RCP 4.5 and RCP 8.5 scenarios.

2 Data and methods

2.1 Model simulations

Daily maximum and minimum temperature data for 2050–2095 were obtained from five simulations and two future scenarios of the EURO-CORDEX project (<http://www.euro-cordex.net>). EURO-CORDEX is the European branch of the international CORDEX initiative, which is a programme sponsored by the World Climate Research Programme (WCRP) to produce regional climate change projections for all terrestrial regions of the world. CORDEX results serve as the basis for climate change impact and adaptation studies within the Intergovernmental Panel on Climate Change (IPCC) (Guilyardi et al. 2011; Taylor et al. 2012; Jacob et al. 2014) (Supplementary Material Table S1). The selection of the RCA4 model in the spatial context of the IPB (Fig. 1) responds to its efficiency in reproducing the climatic conditions of the reference period (1971–2000)

(Strandberg et al. 2014; Kjellström et al. 2016). This climatological normal is the one used by EURO-CORDEX. The spatial resolution provided by EURO-CORDEX for the European region is 0.11° (~12.5 km).

For projecting future temperatures, two RCPs were employed: RCP 4.5 («middle of the way»), representing stabilization of radiative forcing at 4.5 W/m² by the end of this century; and RCP 8.5 («business-as-usual»), the most severe scenario, with a radiative forcing of 8.5 W/m² (Moss et al. 2010; Riahi et al. 2011). RCP 2.6 was not considered as no sufficiently strong climate stabilization actions have been undertaken, and the radiative forcing associated with this scenario has already been surpassed (IPCC 2023; Núñez-Hidalgo et al. 2023). Neither was RCP 6.0, unavailable in EURO-CORDEX simulations. Among the scenarios with high greenhouse gas emission rates, RCP 8.5 is mostly used as the basis for prediction. This is in line with our previous work for the first half of the century (2021–2050) (Lorenzo et al. 2021; Díaz-Poso et al. 2023b).

2.2 Excess heat factor/excess cold factor

Developed by Nairn and Fawcett (2013), the EHF and ECF indices quantify the intensity of heat/cold waves. Because the resulting measure is focused on the intensity, it is possible to identify which events could have severe implications for the population (Nairn and Fawcett 2015; Scalley et al. 2015; Wang et al. 2016). Each index is a factorisation of two daily excess heat/cold indices, and therefore its result is expressed in °C². The first factors are based on a three-day average daily temperature (three-day average daily period, or TDP). The TDP, compared to the 95th percentile (05th) of the average daily temperature of the climatological reference period (1971–2000), constitutes the significance index EHI_{sig} (ECI_{sig}):

$$\begin{aligned} EHI_{sig_i} &= \frac{(T_i + T_{i+1} + T_{i+2})}{3} - T_{95}, \\ ECI_{sig_i} &= \frac{(T_i + T_{i+1} + T_{i+2})}{3} - T_{05}, \end{aligned}$$

where T is the daily mean temperature, i represents each day of the TDP, and $T_{95(05)}$ is the 95th (05th) percentile of daily mean temperature for the study period (Nairn and Fawcett 2013; Wang et al. 2016). When the result of EHI_{sig} is > 0, the three-day period is considered abnormally warm in comparison with the climatology of the study area, indicating a heat wave, whereas negative values (< 0) of ECI_{sig} indicate an abnormally cold period corresponding to a cold wave.

The second component, the acclimatization index EHI_{accl}/ECI_{accl}, is identical for both indices. It quantifies heat/cold stress by comparing the temperatures reached during the TDP considered with those reached in the recent past (mean

temperature of the previous 30 days) (Nairn and Fawcett 2013):

$$\begin{aligned} EHI_{accl_i} &= \frac{(T_i + T_{i+1} + T_{i+2})}{3} - \frac{(T_{i-1} + \dots + T_{i-30})}{30}, \\ ECI_{accl_i} &= \frac{(T_i + T_{i+1} + T_{i+2})}{3} - \frac{(T_{i-1} + \dots + T_{i-30})}{30}. \end{aligned}$$

This acclimatization (EHI_{accl}; ECI_{accl}) is an amplifying factor of the significance index (EHI_{sig}; ECI_{sig}), which in no case reduces the significance of the excess heat/cold of the climatic threshold because $EHI_{accl}(ECI_{accl})$ must be greater than 1 (less than –1). The multiplication of these two factors results in the EHF/ECF indices, of which only EHF (ECF) values greater (less) than 0 can be considered to represent heat wave (cold wave) days:

$$\begin{aligned} EHF_i &= EHI_{sig_i} \cdot \max(1, EHI_{accl_i}), \\ ECF_i &= ECI_{sig_i} \cdot \min(-1, ECI_{accl_i}). \end{aligned}$$

The more positive (negative) the values recorded by EHF (ECF), the more intense will be the phenomena that they measure.

2.3 Statistical analysis

Projections for the second half of the 21st Century (2050–2095) were evaluated using the multi-model ensemble average resulting from the five simulations. Data from the reference period (1971–2000) were used to obtain the climate change signal simulated by RCA4. This signal was obtained using the "delta method" (Zahn and Von Storch 2010) applied at climatological scale. This method's hypothesis is that a "jump" in the mean manifests the signal of climate change, preserving the distribution observed in the present time and showing the differences between the reference and projected periods. Therefore, for all projected values, subtracting the mean of the 1971–2000 reference integration from the mean of the 2050–2095 integration gives us the "delta", with which the percentage change between the values during the reference period and those obtained in the RCP 4.5 and RCP 8.5 scenarios was calculated. The non-parametric two-sided Wilcoxon rank sum test was used to assess whether these changes were significant ($\alpha=0.05$). This test is used to determine whether the distributions of two independent samples are different (Wilcoxon 1945).

Future changes in the EHF/ECF indices were analysed along two main dimensions: intensity (mean and extreme EHF/ECF values) and spatial extent (area corresponding to the number of pixels with positive/negative EHF/ECF values). Only positive (for EHF) and negative values (for ECF) were considered in this analysis. Trend analysis was performed using the non-parametric Mann–Kendall test

with a confidence level of 95% (Mann 1945; Kendall 1975). This test is a widely used method for analysing climate data because it does not require specific data distributions. In agreement with our previous work (Lorenzo et al. 2021; Díaz-Poso et al. 2023b), to illustrate the considerable spatial differences, the main results are shown for the IPB as a whole.

3 Results

3.1 Excess heat factor/excess cold factor trends in 1971–2000

Both EHF and ECF trends showed notable regional differences for the 1971–2000 reference period. The annual average positive EHF (EHF_{mean}) and annual maximum intensity (EHF_{max}) showed similar behaviour, with continental and especially altitudinal effects. The average positive EHF_{mean} value was 6.5°C^2 for the IPB, and the EHF_{max} was 18.53°C^2 (Supplementary Material Figure S1). In addition to the main mountain systems, the western region recorded much higher intensities. The trend was more pronounced for maximum intensity (EHF_{max}), ranging between 2 and 6°C^2 per decade (Supplementary Material Figure S2), than for mean intensity (EHF_{mean}), which ranged between 0 and 2°C^2 per decade. The maximum extent of heat waves increased much faster (4.3%/decade) than the mean annual extent (1.7%/decade) (Supplementary Material Figure S3).

In the same manner, ECF values did not show any latitudinal effect. The highest intensities, both mean (ECF_{mean}) and maximum (ECF_{max}), were recorded in the main mountainous areas, showing a clear dependence on altitude and a similar pattern. ECF_{mean} was -4.7°C^2 , and ECF_{min} was -52.46°C^2 in the IPB (Supplementary Material Figure S4). The eastern half, and especially the northeastern

part of the peninsula, recorded much higher intensities than the western half, in contrast to the pattern observed for EHF. The ECF_{min} trend ranged from -4 to $+9^{\circ}\text{C}^2$ per decade (Supplementary Material Figure S5). The maximum extent of cold waves decreased by $-0.8\%/\text{decade}$, whereas the mean annual extent decreased by $-0.3\%/\text{decade}$ (Supplementary Material Figure S6).

In summary, in the 1971–2000 reference period, the decrease in maximum intensity of cold waves was more pronounced than the increase in maximum intensity recorded for heat waves, although the significant trend corresponds to a much larger extent in the IPB in the case of heat waves. It is also important to highlight the higher rate of increase in the spatial extent (especially the maximum) of heat waves compared to the rate of decrease recorded for cold waves. The results of EHF and ECF for 1971–2000 are summarized in Supplementary Material Table S2.

3.2 Excess heat factor trends in 2050–2095

In the second half of the century, EHF trends continued to show important regional differences, as observed in the 1971–2000 reference period. The differences between the RCP 4.5 and RCP 8.5 scenarios intensified markedly with respect to the first half of the century (Lorenzo et al. 2021; Díaz-Poso et al. 2023b). This was because CO_2 emissions in the RCP 4.5 scenario started to decrease from 2050 onwards (IPCC 2023), whereas the RCP 8.5 scenario reached its maximum radiative forcing at the end of the century (Riahi et al. 2011).

Figure 2 shows the positive annual average EHF intensity (EHF_{mean}) for both scenarios. Greater intensity was recorded in the western and northwestern regions of the peninsula, as well as a marked altitudinal effect. No latitudinal effect was observed, but there was an increase in intensity in the northwest compared to the southeast (RCP 4.5). The average

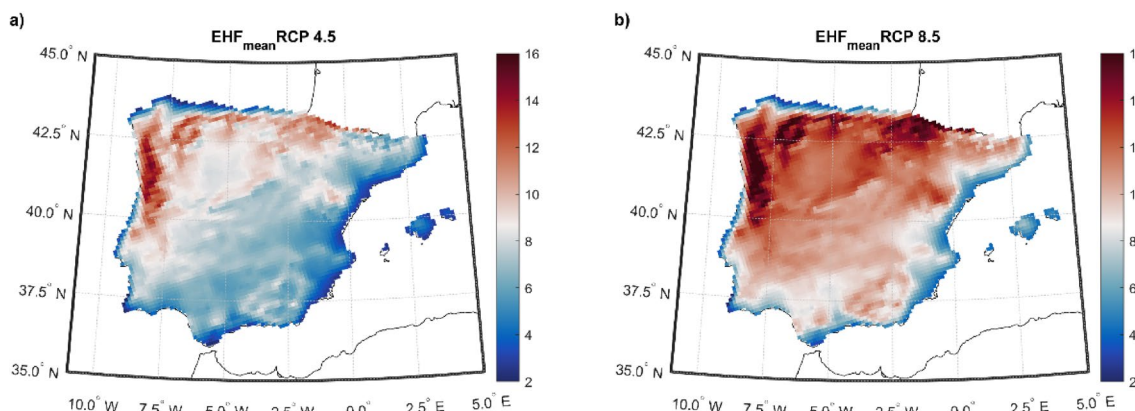


Fig. 2 **a** Annual average positive EHF_{mean} for 2050–2095, RCP 4.5 (average 7.4°C^2); **b** annual average positive EHF_{mean} for 2050–2095, RCP 8.5 (average 10°C^2) (spatial average 8.7°C^2)

intensity between the two scenarios was 8.7°C^2 , representing an increase of more than 50% in the RCP 8.5 scenario with respect to the reference period. The mean intensity was considerably lower in the eastern part of the peninsula, and the lowest values ($2\text{--}4^{\circ}\text{C}^2$) were recorded in coastal areas.

Figure 3 illustrates the spatial distribution of the annual maximum intensity (EHF_{max}). As for EHF_{mean}, the highest intensities are found in the western and northwestern peninsular areas and main elevations of the IPB, especially northern ones. A substantial intensification was observed in RCP 8.5 with respect to the first half of the century (Lorenzo et al. 2021). Whereas in the RCP 4.5 scenario, EHF_{max} values $\geq 40^{\circ}\text{C}^2$ were recorded only in the western and northwestern peninsular areas and main mountainous areas, in the RCP 8.5 scenario, much of the peninsula had values $> 60^{\circ}\text{C}^2$, even exceeding 90°C^2 in the western peninsular area, Leon Mountains, Cantabrian Mountains, and Pyrenees. The spatial mean between both RCPs was 43.18°C^2 . In both RCPs, the lowest intensities, $\leq 25^{\circ}\text{C}^2$, were recorded in the Balearic archipelago, central part of the

Cantabrian coast, and along the Mediterranean coast, with a greater extent towards the interior of the peninsula in the case of the RCP 4.5 scenario.

The EHF_{mean} and EHF_{max} patterns for this period show spatial behaviour like those observed in 1971–2000 and in 2021–2050 (Lorenzo et al. 2021). However, in the case of EHF_{max} under RCP 8.5, the strong increase in intensity implies some blurring of regional differences, as the common mean between both RCPs is comfortably exceeded in most of the IPB (Fig. 3b).

Figure 4 shows the percentage change in EHF_{max} for 2050–2095 compared with 1971–2000. Heat waves will become much more intense in both scenarios, especially in the eastern portion of the IPB. With respect to the historical reference period, in the RCP 8.5 scenario, the maximum intensity of heat waves will triple (200%) in most of the IPB and will quadruple (300%) in several areas of the eastern half of the peninsula. The highest percentages of change were reached in the Pyrenees and in the Iberian System, exceeding 300%. In both scenarios, the smallest

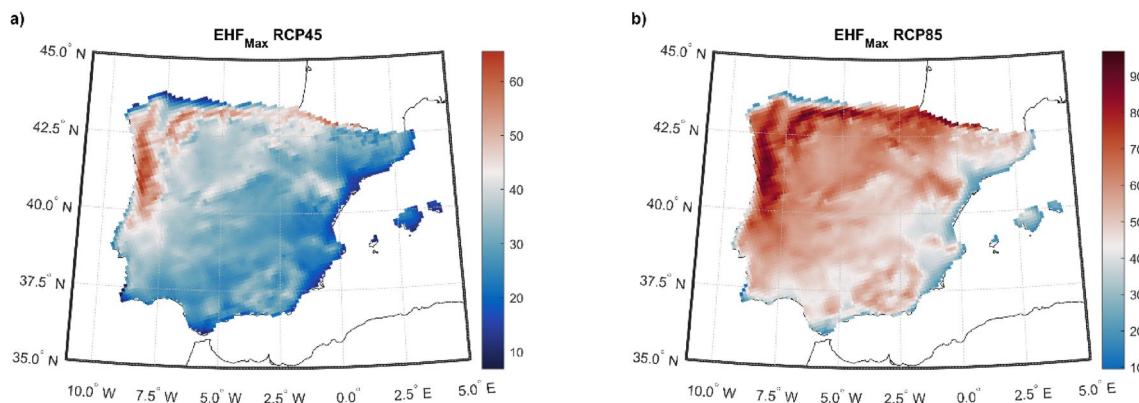


Fig. 3 **a** EHF_{max} for 2050–2095, RCP 4.5 ($^{\circ}\text{C}^2$) (average 32.22°C^2); **b** EHF_{max} for 2050–2095, RCP 8.5 ($^{\circ}\text{C}^2$) (average 53.14°C^2) (spatial average 43.18°C^2)

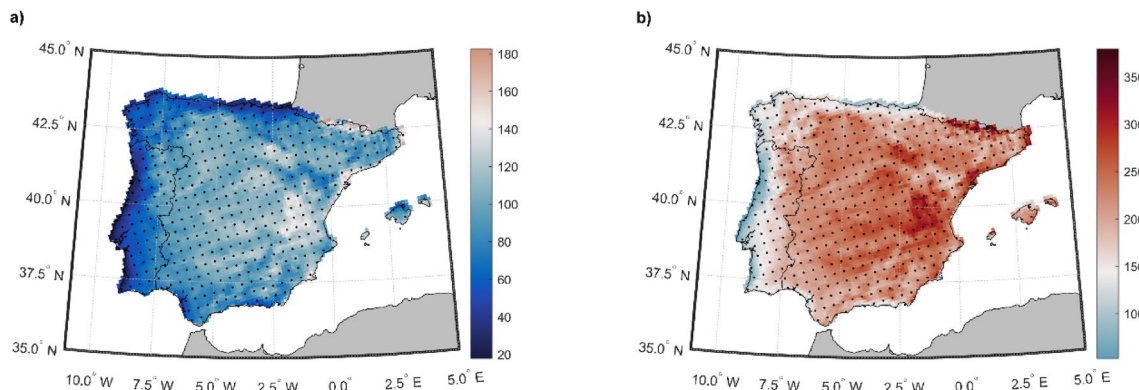


Fig. 4 Percentage change in the maximum value of the EHF index for 2050–2095 compared with 1971–2000 for both scenarios: **a** RCP 4.5 (mean warming of 86.96%); and **b** RCP 8.5 (mean warming of 201.10%). Black dots: significant change at $\alpha=0.05$ (average value is 144%)

increases in intensity occurred along the Cantabrian and Atlantic coasts, ~20%–40% (~50%) under RCP 4.5 (RCP 8.5). The average warming between the two scenarios was 144%.

The EHF_{max} trends for 2050–2095 ranged between –2 to 3 °C²/decade and 2 to 12 °C²/decade for the RCP 4.5 and RCP 8.5 scenarios, respectively (Fig. 5). In RCP 4.5 (Fig. 5a), the negative trend is not significant (~–2 °C²/decade). The rest of the IPB registers positive values, which are significant in the southern half of the peninsula, Balearic Islands, and Pyrenees, where the maximum heat-wave intensity will increase at a rate of 2 to 3 °C²/decade. In the RCP 8.5 scenario, the trend reveals a large increase in maximum intensity for 2050–2095 (Fig. 5b), which is significant across the IPB. The spatial pattern is similar to the percentage change in EHF_{max} (Fig. 4b), with the most pronounced trends in the eastern and northeastern parts of the peninsula (>8 °C²/decade). Particularly noteworthy are the Pyrenees and Iberian System, where the greatest

increases in intensity will occur in the second half of the century (≥ 10 °C²/decade).

The spatial extent of heat waves in the IPB for 2050–2095 is shown in Fig. 6. Heat waves will cover an increasing proportion of the IPB, showing huge differences from the reference period (1971–2000). Whereas in the historical period, the greatest extent has never reached 80%, in 2050–2095, this value will be exceeded in 35 years under RCP 4.5 (76% of years) and in every year under RCP 8.5. Indeed, under this scenario, the upper limit will be approximately 100% of IPB extent from 2077 onwards. 50% of heat waves, represented as the interquartile range (difference between the 75th and 25th percentiles), has also increased greatly compared to the historical period, which shows that heat waves will increasingly affect a larger portion of the IPB. The median is also much higher, exceeding 10% extent in 95% of years for RCP 4.5 and in 100% of years for RCP 8.5. A median exceeding this value was extremely rare in 1971–2000, occurring in only 6% of years.

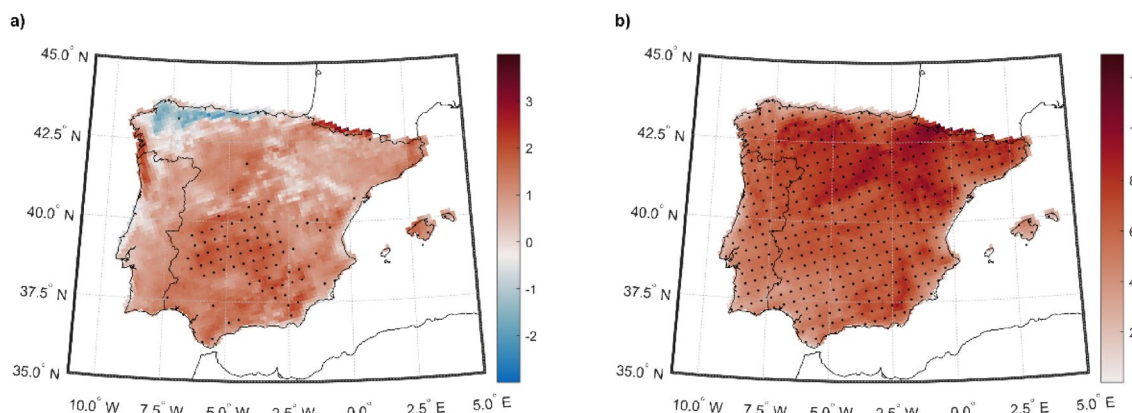


Fig. 5 Trend in the maximum value of the EHF index for 2050–2095 under **a** RCP 4.5 and **b** RCP 8.5. Values are expressed as °C²/decade. Black dots: significant change at $\alpha=0.05$

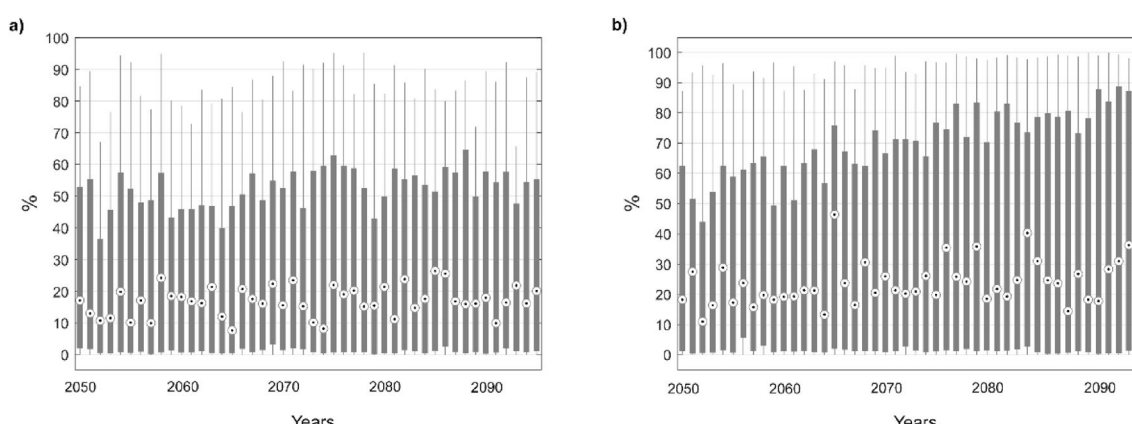


Fig. 6 Distribution of spatial extents of heat waves per year in the Iberian Peninsula and Balearic Islands (2050–2095): **a** RCP 4.5 and **b** RCP 8.5. The point indicates the median, the boxes the interquartile range, and the whiskers the observed range

Although at the beginning of the second half of the century, the projected extents are already very large, there is a positive trend in the mean and maximum annual extents in both scenarios. Between 2050 and 2095, the mean annual extent will increase by 1%/decade for the RCP 4.5 scenario and by 2.7%/decade in the case of RCP 8.5. The increase in maximum annual extent is slightly less, with trends of 0.6%/decade and 2.1%/decade, respectively.

EHF projections for 2050–2095 are summarized and compared to the 2021–2050 period (Lorenzo et al. 2021, 2023b) in Fig. 7. Intensity (EHF_{mean} and EHF_{max}) and extent (mean and maximum) dimensions are included for the RCP 4.5 and RCP 8.5 scenarios. The intensity and spatial extent dimensions of heat waves in the IPB will increase with respect to 2021–2050 in all RCP scenarios. For both periods, and especially for 2050–2095, the RCP 8.5 scenario differs considerably in terms of magnitude from the RCP 4.5 scenario.

The median values of EHF_{mean} show approximately equal values in the RCP 4.5 scenario for both periods ($7.24\text{ }^{\circ}\text{C}^2$ in 2050–2095; $6.65\text{ }^{\circ}\text{C}^2$ in 2021–2050), but differ more widely from each other in the RCP 8.5 scenario ($9.76\text{ }^{\circ}\text{C}^2$ in 2050–2095; $7.87\text{ }^{\circ}\text{C}^2$ in 2021–2050). For EHF_{max}, the differences between the two periods are markedly accentuated, especially in RCP 8.5, where the median value will double ($53.27\text{ }^{\circ}\text{C}^2$ in 2050–2095; $23.78\text{ }^{\circ}\text{C}^2$ in 2021–2050).

The mean extent shows almost equal values between periods for the RCP 4.5 scenario, but a larger difference for RCP 8.5 (35.72% in 2050–2095; 31.61% in 2021–2050). The differences in extent reach their greatest degree at the

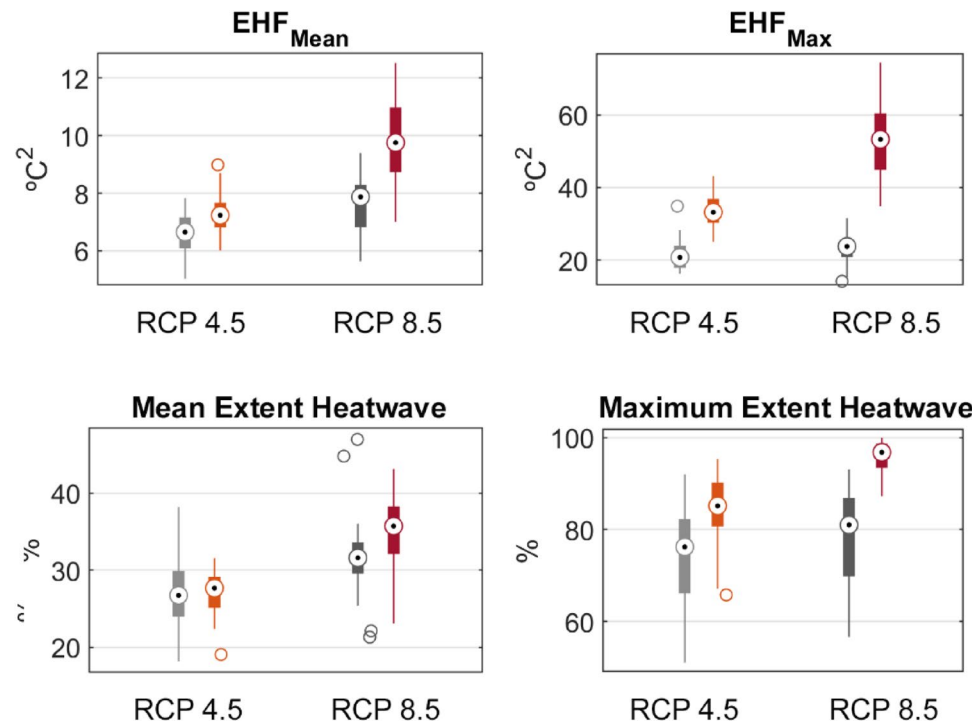
maximum, with differences at the median of 9% for RCP 4.5 and 16% for RCP 8.5 (96.8% in 2050–2095; 81% in 2021–2050). The main results of EHF for 2050–2095 are summarized in Supplementary Material Table S3.

3.3 Excess cold factor trends in 2050–2095

Regional variability is also present for ECF. The annual average negative ECF intensity (ECF_{mean}) for 2050–2095 is shown in Fig. 8 for both scenarios. The low ECF_{mean} values, corresponding to high average intensity, are similarly distributed in both scenarios. No relevant latitudinal influence is observed, as in 1971–2000. The eastern and northeastern peninsular areas stand out ($\leq -6\text{ }^{\circ}\text{C}^2$), as well as the main IPB elevations ($\leq -10\text{ }^{\circ}\text{C}^2$). The decrease in mean annual intensity is considerable with respect to the reference period, with a spatial mean between the two scenarios of $-3.1\text{ }^{\circ}\text{C}^2$, which represents a decrease of 34%.

Figure 9 shows the distribution of annual maximum intensity (ECF_{min}) for both scenarios. In the second half of the century, cold waves are expected to be much less intense in the IPB for both scenarios (mean between the two RCPs: $-23.48\text{ }^{\circ}\text{C}^2$) than in the reference period (mean between the two RCPs: $-52.46\text{ }^{\circ}\text{C}^2$). Conversely, the maximum intensity for the IPB will be higher in the RCP 8.5 scenario ($-24.54\text{ }^{\circ}\text{C}^2$) than in RCP 4.5 ($-22.44\text{ }^{\circ}\text{C}^2$). In contrast to the RCP 4.5 scenario, a slight increase in intensity will be experienced under the RCP 8.5 scenario with respect to the first half of the century (Díaz-Pozo et al. 2023b). In both scenarios, the same spatial pattern as in

Fig. 7 Summary of EHF projections as box-and-whisker plots for IPB in 2021–2050 (greys) and 2050–2095 (orange and red). The point indicates the median, the boxes the interquartile range, and the whiskers the observed range



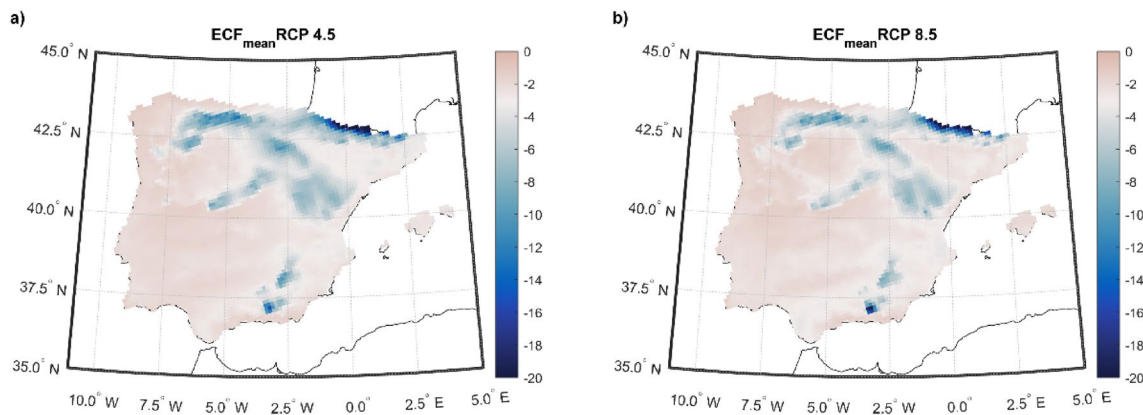


Fig. 8 **a** Annual average negative ECF_{mean} for 2050–2095, RCP 4.5 (average -3.2°C^2); **b** annual average ECF_{mean} for 2050–2095, RCP 8.5 (average -2.9°C^2) (spatial average -3.1°C^2)

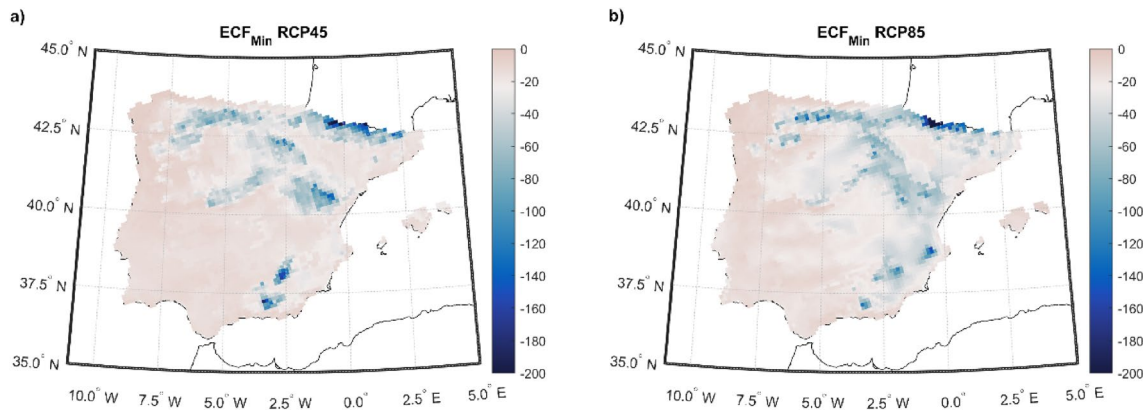


Fig. 9 **a** ECF_{min} for 2050–2095, RCP 4.5 ($^{\circ}\text{C}^2$) (average -22.44°C^2); **b** ECF_{min} for 2050–2095, RCP 8.5 ($^{\circ}\text{C}^2$) (average -24.54°C^2) (spatial average -23.48°C^2)

ECF_{mean} is observed, with higher intensities in the northern and northeastern peninsular regions ($<-50^{\circ}\text{C}^2$), and especially in mountainous systems regardless of their latitude. The Pyrenees stand out ($<-180^{\circ}\text{C}^2$), and to a lesser extent the Cantabrian Mountains, Iberian System, and Betic System ($\leq-100^{\circ}\text{C}^2$). Likewise, in the foothills of the main elevations, the intensities are higher than in the rest of the peninsula. The lowest maximum intensities are recorded in the western and especially the southwestern portions of the peninsula, as well as in coastal areas ($<-20^{\circ}\text{C}^2$).

The spatial patterns of ECF_{mean} and ECF_{min} for this period show a strong altitudinal dependence. The continental effect is less relevant, with a greater influence in the northern sub-plateau than in the southern one due to its higher average altitude. There is no latitudinal effect. Note that the spatial behaviour is similar to the ones observed in 1971–2000 and in 2021–2050 (Díaz-Poso et al. 2023b).

The percentage change in ECF_{min} is shown in Fig. 10. Cold waves will be less intense in the second half of the

century than in the reference period. The percentage change is significant across the entire IPB. In both scenarios, warming is slightly more pronounced in the northern half of the peninsula ($<-50\%$), regardless of altitude. The average warming in the RCP 8.5 scenario will be lower. In this scenario, with higher-magnitude intensities (Fig. 9b), there is greater warming in the northern third of the peninsula, as well as an increase in the intensity of cold waves on both plateaus ($\leq 50\%$). Locally, at the eastern end of the Betic System (Fig. 1), increases ranging between 150 and 200% with respect to the historical reference period will occur. The mean ECF_{min} warming between the two scenarios will be 15.85%.

The ECF_{min} trends for 2050–2095 are shown in Supplementary Material Figure S7 for both scenarios. For RCP 4.5, trends range between $3^{\circ}\text{C}^2/\text{decade}$ and $-2^{\circ}\text{C}^2/\text{decade}$. The most notable negative trends (corresponding to an increase in intensity) are mainly recorded in the southern foothills of mountain systems such as the Central System or Betic

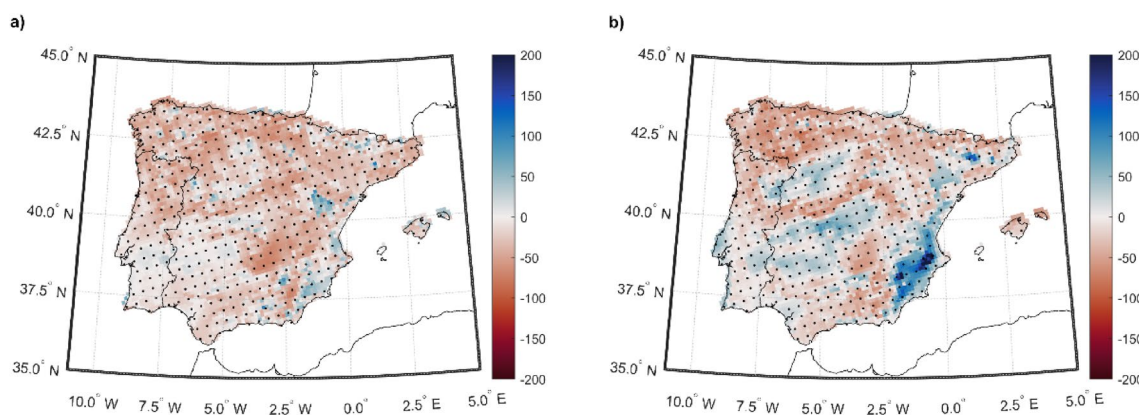


Fig. 10 Percentage change in the minimum ECF index for 2050–2095 compared with 1971–2000 for both scenarios: **a** RCP 4.5 (mean warming of 21.6%); and **b** RCP 8.5 (mean warming of 10.1%). Black dots: significant change at $\alpha=0.05$

System ($\sim -2^{\circ}\text{C}^2/\text{decade}$), although they are not significant. The main positive trends ($2\text{--}3^{\circ}\text{C}^2/\text{decade}$), occupy a greater extent, being registered in the Leon Mountains, Cantabrian Mountains, Iberian System, and occasionally the Central System and Pyrenees, but they are not significant. Significant decreases in intensity are moderate ($0\text{--}1^{\circ}\text{C}^2/\text{decade}$) and are confined to small areas in the northwestern part of the peninsula. Under RCP 8.5, trends are recorded in very small mountain areas, and none are significant. Positive trends are recorded in the Iberian System, Cantabrian Mountains, and Leon Mountains. In general terms, negative trends are only observed in very small areas of the Pyrenees. Therefore, in the second half of the 21st Century, there will be no significant relevant trend because the 2050s will start from maximum intensity values of lesser magnitude, which will remain approximately similar until the end of the century.

The distribution of the annual extent of cold waves in the IPB for 2050–2095 is represented in Fig. 11. Whereas

in 1971–2000, the upper boundary extent exceeded 30% of the IPB in 21 years (70% of years), in the second half of the century, it will be exceeded only twice in the RCP 4.5 scenario (4.35% of years) and not at all in RCP 8.5. In this scenario, the greatest extent will not reach 20% of the IPB extent in any year; in the historical period, this has been an extraordinary event, occurring in only one year. 50% of cold waves, represented as the interquartile range (the difference between the 75th and 25th percentiles), show how half the cold waves will have a much smaller spatial extent than they did in 1971–2000, especially in RCP 8.5. Although very infrequent, extensive cold waves may also occur, as shown by the outliers, covering more than 40% and 30% of the IPB extent in the RCP 4.5 and RCP 8.5 scenarios, respectively.

Although at the beginning of the second half of the century the predicted extents are already low, future trends show a decrease in the mean extent of cold waves of $-0.1\%/\text{decade}$ for the RCP 4.5 scenario and -0.5% for RCP 8.5, with

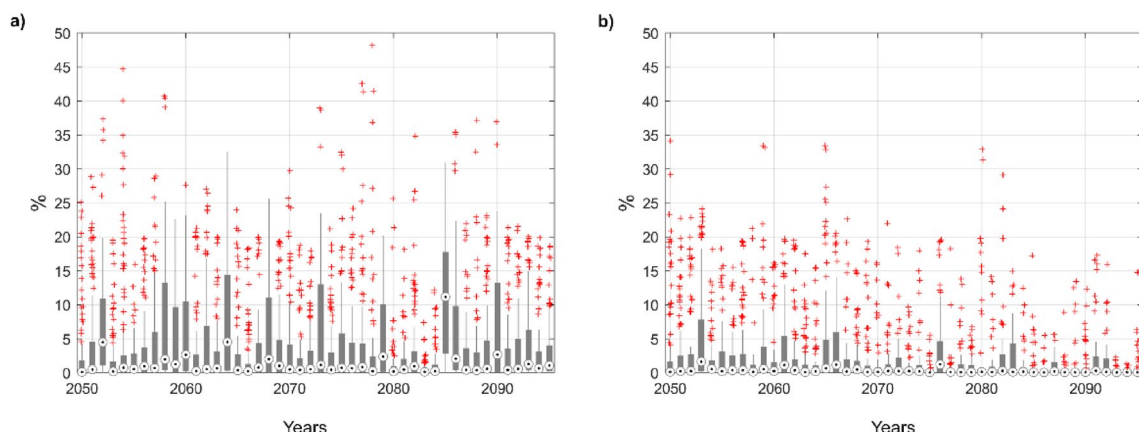


Fig. 11 Distribution of spatial extents of cold waves per year in the Iberian Peninsula and Balearic Islands (2050–2095): **a** RCP 4.5; and **b** RCP 8.5. The point indicates the median, the boxes the interquartile range, and the whiskers the observed range

the negative trend being more accentuated in the maximum extents, which decrease by -0.7% and -3.2% per decade, respectively. The negative trend obtained for the RCP 8.5 scenario shows a decrease of much greater magnitude than that recorded for the RCP 4.5 scenario, which is associated with a much more restricted anthropogenic radiative forcing (8.5 W/m^2 and 4.5 W/m^2 , respectively).

Finally, Fig. 12 shows the ECF projections for 2050–2095 summarized and compared to the first half of the century (2021–2050) (Díaz-Poso et al. 2023b). Intensity (ECF_{mean} and ECF_{min}) and extent (mean and maximum) are included for the RCP 4.5 and RCP 8.5 scenarios. The differences between periods are considerably reduced compared to those observed for heat waves (Fig. 7). Only one exception is observed: a greater difference between periods in the average extent of cold waves (RCP 4.5). The largest inter-period differences are clearly observable in the RCP 8.5 scenario. The median values of intensity and extent will not increase in magnitude with respect to 2021–2050 in any scenario.

The median value of ECF_{mean} will be practically the same for both periods in the RCP 4.5 scenario ($-2.59 \text{ }^\circ\text{C}^2$ in 2050–2095; $-2.61 \text{ }^\circ\text{C}^2$ in 2021–2050), with the median value increasing slightly in RCP 8.5 for the second half of the century ($-2.35 \text{ }^\circ\text{C}^2$ in 2050–2095; $-3.49 \text{ }^\circ\text{C}^2$ in 2021–2050). ECF_{min} shows that the differences between periods will remain moderate for the RCP 4.5 scenario and will be accentuated in RCP 8.5, increasing the median and minimum values in the second half of the century ($-4.21 \text{ }^\circ\text{C}^2$; $-16.04 \text{ }^\circ\text{C}^2$) with respect to 2021–2050

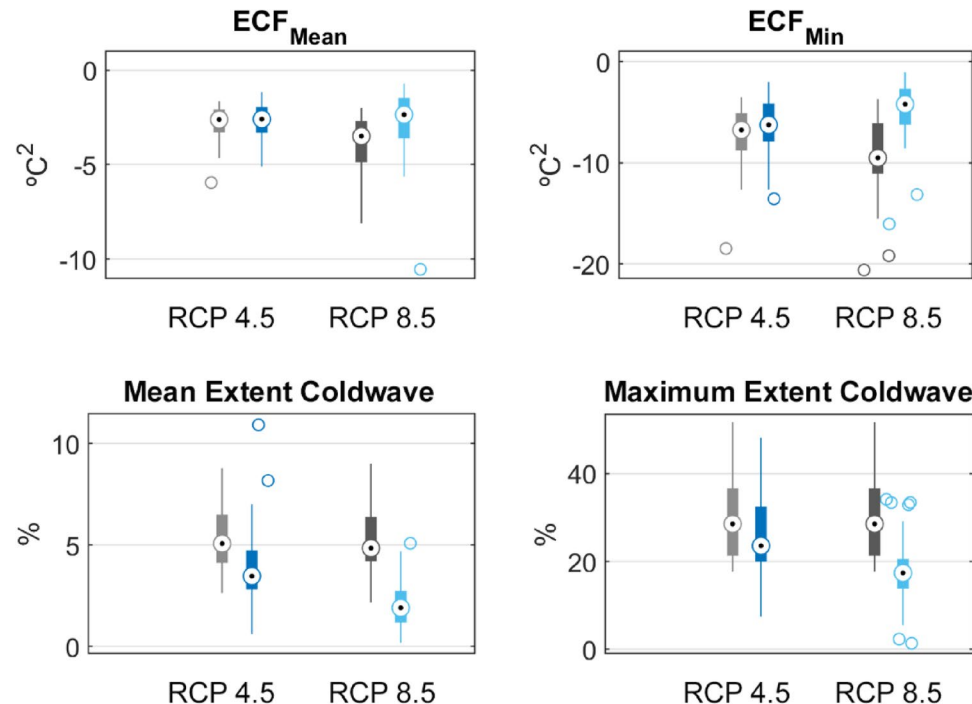
($-9.51 \text{ }^\circ\text{C}^2$; $-20.58 \text{ }^\circ\text{C}^2$). The variability will be much greater for ECF_{min} than for ECF_{mean}.

The mean extent shows a more marked difference between periods than that observed for intensity. The median value in the RCP 8.5 scenario for 2050–2095 will be reduced by $\sim 3\%$ compared to 2021–2050 (1.91% and 4.85% , respectively). In the case of the maximum extent of cold waves, the median value will be reduced for 2050–2095 by 11.85% in RCP 8.5 (17.38% for 2050–2095 and 29.23% for 2021–2050). The variability, as shown by the upper and lower limits, will be much higher for the maximum extent than for the mean extent, especially for RCP 4.5, with expected ranges of 48.19% and 7.42% , respectively. The main results of ECF for 2050–2095 are summarized in Supplementary Material Table S3.

4 Discussion

This study extends to the second half of the century the analysis of the intensity of future heat and cold waves in the IPB using the EHF and ECF indices proposed by Lorenzo et al. (2021) and Díaz-Poso et al. (2023b) for the first half of the century. The two main dimensions, intensity and spatial extent, are addressed using 1971–2000 as the historical reference period and 2050–2095 as the future period. The RCP 4.5 and RCP 8.5 scenarios have been used to quantify the differential behaviour between the respective radiative forcings at the end of the century. Knowing this differential behaviour will lead us to

Fig. 12 Summary of ECF projections as box-and-whisker plots for IPB in 2021–2050 (greys) and 2050–2095 (blues). The point indicates the median, the boxes the interquartile range, and the whiskers the observed range



a deeper understanding of the intensity of future extreme temperature events.

The results show how the spatial patterns of mean and maximum EHF intensity in 1971–2000 will be repeated for 2050–2095. The highest intensities are recorded in the western part of the peninsula and at the higher mountainous elevations. This intensity distribution is due to the presence at altitude of the North African ridge, which implies an injection of very warm air into the upper layers of the atmosphere, which triggers most of the heat waves affecting the IPB (Merino et al. 2018; Sousa et al. 2019; Lorenzo et al. 2021; Díaz-Poso et al. 2023a). Likewise, the lower intensity in the eastern peninsular region, and more specifically along the Mediterranean coast and in the Balearic Islands, is a response to the loss of energy of the North African continental tropical air mass in its advection process over the Mediterranean Sea (Díaz-Poso et al. 2023a).

The difference between scenarios will be more marked in 2050–2095 than in 2021–2050 (Lorenzo et al. 2021) because in the RCP 4.5 scenario, emissions will start to decrease in 2050, whereas in the RCP 8.5 scenario, the highest radiative forcing will be reached at the end of the century (Riahi et al. 2011; IPCC 2023). This is reflected in the EHF_{\max} values for both scenarios. Under RCP 8.5, most of the IPB records values $> 60 \text{ }^{\circ}\text{C}^2$, whereas in RCP 4.5, such values are confined only to the northern mountainous areas and the northwestern fringe, where the influence of the North African ridge is greatest.

The results show the same trends for heat waves in 2050–2095 as in the first half of the century (Lorenzo et al. 2021). For instance, the RCP 8.5 scenario shows the highest increments in EHF_{\max} , with a percentage change of 100% along the Mediterranean coast, in the Iberian System, and in the Pyrenees with respect to 2021–2050 (Lorenzo et al. 2021). These results point to the same direction as the latest works that have used the EHF index in the IPB (Royé et al. 2020; Espín-Sánchez and Conesa-García, 2021; Oliveira et al. 2022; Díaz-Poso et al. 2023a; Khodayar and Paredes-Fortuny, 2023; Paredes-Fortuny and Khodayar 2023).

The EHF projections also show how the spatial extent of heat waves will continue to increase (Keellings and Moradkhani 2020; Sánchez-Benítez et al. 2020; Khodayar and Paredes-Fortuny, 2023; Paredes-Fortuny and Khodayar 2023). However, trends are considerably lower than that recorded in the reference period or that expected for the first half of the century in the RCP 4.5 scenario (Lorenzo et al. 2021). These values can be explained by the fact that the assumed reduction in emissions achieved in the first half of the century stabilises the CO_2 concentration in the atmosphere and prevents heat waves from becoming more extreme. In the RCP 8.5 scenario, the reason for a lower trend value is that the scenario is so extreme that from 2077

onwards, the maximum value for the extent of heat waves is approximately 100%.

Our results show how all the dimensions analysed for heat waves will increase in the second half of the century compared to 1971–2000 and 2021–2050, with a more pronounced difference between scenarios. These results agree with studies that have analysed heat waves for the end of the century in the IPB and the Mediterranean Region (Pereira et al. 2017; Viceto et al. 2019; Molina et al. 2020; Zittis et al. 2022).

For cold waves, the results show that the spatial pattern of mean and minimum ECF in 1971–2000 will also be repeated for 2050–2095. Intensities will be higher in the eastern and northeastern portions of the peninsula, as well as in the main mountain systems. The lowest intensities will be recorded in the western and southwestern regions of the peninsula and in coastal areas. This distribution pattern is a response to the presence of a trough at 500 hPa over the northeastern portion of the IPB, which conducts an extremely cold continental air mass into the eastern and northeastern regions of the Iberian Peninsula. This pattern gives rise to most of the cold waves affecting the IPB (Mohammed et al. 2018; Serrano-Notívoli et al. 2022; Díaz-Poso et al. 2023b).

The maximum and average intensities for both scenarios will be much lower than those reported in the historical period. In general terms, for both ECF_{mean} and ECF_{\min} , there is an directly proportional dependence between intensity and height, with no latitudinal influence. In both ECF_{\min} scenarios, the highest intensities are reached in the Pyrenees, Cantabrian Mountains, Iberian System, and Betic System. We find that the maximum intensity (ECF_{\min}) for the IPB will be higher in the RCP 8.5 scenario than in the RCP 4.5 scenario, even slightly exceeding the average of its counterpart scenario for 2021–2050.

Therefore, in terms of maximum intensity, there will not be as much difference between scenarios as in the case of heat waves, and even under large radiative forcing (RCP 8.5), there will be wide variability in the occurrence of these extreme phenomena (Kodra et al. 2011). This finding is in complete contrast to that of Smid et al. (2019), who predicted that cold waves would disappear completely by the end of the century. The use of the Cold Wave Magnitude Index daily (CWMId), which is less sensitive than the ECF to local temperature variations and therefore less effective at detecting cold waves that are not solely characterized by an extreme minimum temperature, could explain the discrepancy between results. No significant trends are observed in the maximum intensity, given that from the 2050s, ECF_{\min} values will remain approximately similar until the end of the century.

ECF projections show negative trends in extent for the second half of the century. These trends are not very noticeable because the average extent of cold waves in 2050 will

correspond to a very low percentage of the IPB. In both scenarios, the decrease in maximum extent is considerably less than that registered in the first half of the century (Díaz-Poso et al. 2023b).

These results are consistent with work that has addressed the dimensions of intensity and extent in recent decades at the European/IPB level, both with the ECF index (Piticar et al. 2018; Espín-Sánchez and Conesa-García 2021) and with other indices (Spinoni et al. 2015; Van Oldenborgh et al. 2019; Serrano-Notívoli et al. 2022). The projected decreases are also in agreement with the few projections that include cold waves for the second half of the century (Pereira et al. 2017; King and Karoly 2017; Viceto et al. 2019).

Given the vulnerability of the Mediterranean region (MedECC 2020; Urdiales-Flores et al. 2023) and specifically of the IPB, these future increases will imply a greater impact on the health of an increasingly aging population (Chen 2024), a greater risk of fires, and greater energy expenditure. This highlights that adaptation and mitigation strategies will inevitably have to be improved and adapted to each region because, as has been shown, heat-wave intensity will vary greatly throughout the IPB, affecting each region in very different ways. In this sense, the greater sensitivity of the index to local temperature variations (Díaz-Poso et al. 2023a) and the possibility of using it predictively may be especially useful in decision-making processes such as declaring or maintaining a health alert.

The current reduction in cold-related mortality due to rising temperatures (Wang et al. 2016; Gasparini et al. 2017) will give way to an increase in the future due to an aging population, which in turn will be acclimatized to higher temperatures (Vardoulakis et al. 2014; Ordanovich et al. 2023; Chen 2024) and will be highly vulnerable to cold waves (Gasparini et al. 2015; Carmona et al. 2016; Vicedo-Cabrera et al. 2018). Likewise, the impacts on mortality will also be conditioned by the sequence of occurrence of heat and cold waves. A particularly intense heat or cold wave could cause an initial excess mortality among the most vulnerable groups, which could attenuate the impact on mortality of subsequent events by reducing the proportion of individuals in a high-risk situation within the population. In a context of less frequent cold waves, all of this could imply a decrease in risk perception and adaptation measures (Pinto et al. 2024), which could pose a major threat to the health of the population because, as we have found, cold waves will continue to occur in the second half of the century, even in the RCP 8.5 scenario of much greater warming. It will therefore be necessary to establish and develop regional response plans for cold waves. For the same reasons as its analogue for heat waves, the ECF index has proven to be a useful tool in making decisions regarding health warnings for cold waves.

5 Conclusions

We have performed an analysis of the intensity and extent of heat and cold waves in the IPB for the second half of the century (2050–2095) under the RCP 4.5 and RCP 8.5 scenarios using the EHF and ECF indices. This analysis is a continuation of the work carried out for the first half of the century by Lorenzo et al. (2021) and Díaz-Poso et al. (2023b). The main conclusions are the following:

- The analysed dimensions of intensity and spatial extent will increase(decrease) in magnitude for EHF(ECF) in the second half of the century, with the difference between RCP scenarios being markedly accentuated.
- The highest EHF intensities will be recorded in the western portion of the peninsula and in mountainous areas. The eastern half of the peninsula, and specifically the Mediterranean coast, will record lower intensities.
- The average increase in EHF_{\max} in the IPB will be 144%. The highest percentage changes in EHF_{\max} will be recorded in the eastern and northeastern peninsular region (300%, RCP 8.5), where the trend for 2050–2095 will also be higher ($8\text{--}10^{\circ}\text{C}^2$, RCP 8.5). These percentage changes will be double those foreseen for 2021–2050.
- Due to the magnitude of the maximum extent of mid-century heat waves, the mean extent will increase at a faster rate (1%/decade and 2.7%/decade for RCP4.5 and RCP8.5, respectively) than the maximum (0.6%/decade and 2.1%/decade for RCP4.5 and RCP8.5, respectively).
- The highest ECF intensities will be recorded in the northern and northeastern parts of the peninsula and in mountainous regions. In the western and southwestern parts of the peninsula and in coastal areas, cold waves will have lower intensity.
- The average decrease in maximum cold wave intensity in the IPB will be 16%. This decrease will be lower in the RCP 8.5 scenario and its variability greater, with more marked decreases as well as local increases in intensity.
- The maximum extent of cold waves will continue to decrease by much more than the average extent, with decreases ranging from -0.7/decade to -3.2/decade .
- For both EHF_{\max} and ECF_{\min} , the intensity for the IPB in the RCP 8.5 scenario will be higher than that recorded for 2021–2050.
- The differences between scenarios for 2050–2095 will be much more notable for EHF than for ECF. In addition, except for the mean extent for RCP 4.5, the differences from 2021–2050 will also be larger for EHF, where all dimensions increase in magnitude.

The results show the functionality of the EHF/ECF indices in analysing dimensions of heat and cold waves such as intensity and spatial extent. Analysing the behaviour of these dimensions under two RCP scenarios enables us to quantify the differential evolution of these dimensions by the end of the century. The progress shown in understanding the intensity of future heat and cold waves will be useful for future mitigation and adaptation strategies. The possibility of providing anticipatory information on the intensity of heat and cold waves to public administrations, and specifically to health systems, will minimise the negative effects of these events on the health of the population, as well as their impacts on agriculture, energy, and transport systems. This research is expected to continue in the future. When the new CMIP6-CORDEX datasets with updated state-of-the-art regional climate data become available, projections will be more accurate due to more advanced aerosol forcing modelling, cloud feedbacks, and a more recent reference period (up to 2014), enabling a better assessment of the phenomena analysed here will be possible.

Supplementary Information The online version contains supplementary material available at <https://doi.org/10.1007/s00382-025-07699-4>.

Acknowledgements Alejandro Díaz-Poso is grateful for the support of the FPU programme of the Ministry of Universities [contract number FPU20-04454]. The presented work was partially supported by Xunta de Galicia under project ED431C 2021/44 (Grupos de Referencia Competitiva), Ministerio de Ciencia e Innovación with funding from European Union NextGenerationEU (PRTR-C17.I3) under project TED2021-129152B-C43.

Author contributions All authors contributed to the study conception, design, formal analysis, investigation, methodology and writing. All authors read and approved the final manuscript.

Funding Open Access funding provided thanks to the CRUE-CSIC agreement with Springer Nature. The authors declare that no funds, grants, or other support were received during the preparation of this manuscript.

Data availability The datasets generated during the current study are available from the corresponding author on reasonable request.

Declarations

Conflict of interest The authors have no relevant financial or non-financial interests to disclose.

Open Access This article is licensed under a Creative Commons Attribution 4.0 International License, which permits use, sharing, adaptation, distribution and reproduction in any medium or format, as long as you give appropriate credit to the original author(s) and the source, provide a link to the Creative Commons licence, and indicate if changes were made. The images or other third party material in this article are included in the article's Creative Commons licence, unless indicated otherwise in a credit line to the material. If material is not included in the article's Creative Commons licence and your intended use is not permitted by statutory regulation or exceeds the permitted use, you will need to obtain permission directly from the copyright holder. To view a copy of this licence, visit <http://creativecommons.org/licenses/by/4.0/>.

References

- Acero FJ, Fernández-Fernández MI, Sánchez-Carrasco VM, Parey S, Hoang TTH, Dacunha-Castelle D, García JA (2017) Changes in heat wave characteristics over Extremadura (SW Spain). *Theor Appl Climatol* 133:605–617. <https://doi.org/10.1007/s00704-017-2210-x>
- Añel JA, Fernández-González M, Labandeira X, López-Otero X, De la Torre L (2017) Impact of cold waves and heat waves on the energy production sector. *Atmosphere* 8(11):209. <https://doi.org/10.3390/atmos8110209>
- Baccini M, Biggeri A, Forsberg B, Medina S, Paldy A, Rabchenko D, Schindler C, Michelozzi P, Accetta G, Kosatsky T, Katsouyanni K, Analitis A, Anderson H, Bisanti L, D'Ippoliti D, Danova J (2008) Hot effects on mortality in 15 European cities. *Epidemiology* 19(5):711–719. <https://doi.org/10.1097/ede.0b013e318176bfcd>
- Ballester J, Quijal-Zamorano M, Méndez Turrubiates RF, Pegenaute F, Herrman FR, Robine JM, Tonne C, Antó JM, Achebak H (2023) Heat-related mortality in Europe during the summer of 2022. *Nat Med* 29:1857–1866. <https://doi.org/10.1038/s41591-023-02419-z>
- Barriopedro D, Sousa PM, Trigo RM, García-Herrera R, Ramos AM (2020) The exceptional Iberian heatwave of Summer 2018. *Bull Am Meteorol Soc* 101(1):S29–S33. <https://doi.org/10.1175/BAMS-D-19-0159.2>
- Barriopedro D, García-Herrera R, Ordóñez C, Miralles DG, Salcedo-Sanz S (2023) Heat waves: physical understanding and scientific challenges. *Rev Geophys*. <https://doi.org/10.1029/2022RG000780>
- Bitencourt DP, Fuentes MV, Franke AE, Silveira RB, Alves MP (2019) The climatology of cold and heat waves in Brazil from 1961 to 2016. *Int J Climatol* 40(4):2464–2478. <https://doi.org/10.1002/joc.6345>
- Carmona R, Díaz J, Mirón JJ, Ortíz C, León I, Linares C (2016) Geographical variation in relative risks associated with cold waves in Spain: the need for a cold wave prevention plan. *Environ Int* 88:103–111. <https://doi.org/10.1016/j.envint.2015.12.027>
- Carvalho D, Cardoso Pereira S, Rocha A (2021) Future surface temperatures over Europe according to CMIP6 climate projections: an analysis with original and bias-corrected data. *Clim Change* 167:10. <https://doi.org/10.1007/s10584-021-03159-0>
- Chen K, de Schrijver E, Sivaraj S, Sera F, Scovronick N, Jiang L, Royé D, Lavigne E, Kysely J, Urban A, Schneider A, Huber V, Madureira J, Mistry MN, Cvijanovic I, MCC Collaborative Research Network, Gasparrini A, Vicedo-Cabrera A (2024) Impact of population aging on future temperature-related mortality at different global warming levels. *Nat Commun* 15:1796. <https://doi.org/10.1038/s41467-024-45901-z>
- Copernicus (2023a) Global climate highlights 2023. Copernicus. <https://climate.copernicus.eu/global-climate-highlights-2023>, Accessed 30 Jan 2024
- Copernicus (2023b) Climate indicators: temperature. Copernicus. <https://climate.copernicus.eu/climate-indicators/temperature>, Accessed 31 Jan 2024
- Cos J, Doblas-Reyes F, Jury M, Marcos R, Bretonnière PA, Samsó M (2022) The Mediterranean climate change hotspot in the CMIP5 and CMIP6 projections. *Earth Syst Dyn* 13:321–340. <https://doi.org/10.5194/esd-13-321-2022>
- D'Ippoliti D, Michelozzi P, Marino C, de Donato F, Menne B, Katsouyanni K, Kirchmayer U, Analitis A, Medina-Ramón M, Paldy A, Atkinson R, Kovats S, Bisanti L, Schneider A, Lefranc A, Iñiguez C, Perucci CA (2010) The impact of heat waves on mortality in 9 European cities: Results from the EuroHEAT project. *Environ Health* 9:37. <https://doi.org/10.1186/1476-069X-9-37>

- Díaz-Poso A, Lorenzo N, Royé D (2023a) Spatio-temporal evolution of heat wave severity and expansion across the Iberian Peninsula and Balearic Islands. *Environ Res* 217:114864. <https://doi.org/10.1016/j.envres.2022.114864>
- Díaz-Poso A, Lorenzo N, Martí A, Royé D (2023b) Cold wave intensity on the Iberian Peninsula: future climate projections. *Atmos Res* 295:107011. <https://doi.org/10.1016/j.atmosres.2023.107011>
- Diffenbaugh NS, Pal JS, Giorgi F, Gao X (2007) Heat stress intensification in the Mediterranean climate change hotspot. *Geophys Res Lett.* <https://doi.org/10.1029/2007GL030000>
- Domeisen DIV, Eltahir EAB, Fischer EM, Knutti R, Perkins-Kirkpatrick SE, Schär C, Seneviratne SI, Weisheimer A, Wernli H (2023) Prediction and projection of heatwaves. *Nat Rev Earth Environ* 4:36–50. <https://doi.org/10.1038/s43017-022-00371-z>
- Berkeley Earth (2024) Global temperature report for 2023. Berkeley Earth. www.berkeleyearth.org/global-temperature-report-for-2023. Accessed 30 Jan 2024
- Espín-Sánchez D, Conesa-García C (2021) Spatio-temporal changes in the heatwaves and coldwaves in Spain (1950–2018): influence of the East Atlantic Pattern. *Geogr Pannonica* 25:168–183. <https://doi.org/10.5937/gp25-31285>
- Feng X, Qian C, Materia S (2022) Amplification of the temperature seasonality in the Mediterranean region under anthropogenic climate change. *Geophys Res Lett* 49:1–10. <https://doi.org/10.1029/2022GL099658>
- Fischer EM, Schär C (2009) Future changes in daily summer temperature variability: driving processes and role for temperature extremes. *Clim Dyn* 33:917–935. <https://doi.org/10.1007/s00382-008-0473-8>
- Fischer E, Schär C (2010) Consistent geographical patterns of changes in high-impact European heatwaves. *Nature Geosci* 3:398–403. <https://doi.org/10.1038/ngeo866>
- Gao Y, Huang W, Zhao Q, Rytí N, Armstrong B, Gasparrini A et al (2024) Global, regional, and national burden of mortality associated with cold spells during 2000–19: a three-stage modelling study. *Lancet Planet Health* 8:e108–e116. [https://doi.org/10.1016/S2542-5196\(23\)00277-2](https://doi.org/10.1016/S2542-5196(23)00277-2)
- García-Herrera R, Díaz J, Trigo RM, Luterbacher J, Fischer EM (2010) A review of the European summer heatwave of 2003. *Crit Rev Environ Sci Technol* 40:267–306. <https://doi.org/10.1080/1064380802238137>
- Gasparrini A, Guo Y, Hashizume M, Lavigne E, Zanobetti A, Schwartz J, Tobías A, Tong S, Rocklöv J, Forsberg B, Leone M, De Sario M, Bell ML, Guo YLL, Wu GF, Kan H, Yi SM, de Sousa Zanotti Staglilio Coelho M, Nascimento Saldiva PH, Honda Y, Kim H, Armstrong B (2015) Mortality risk attributable to high and low ambient temperature: a multicountry observational study. *Lancet* 386(9991):369–375. [https://doi.org/10.1016/S0140-6736\(14\)62114-0](https://doi.org/10.1016/S0140-6736(14)62114-0)
- Gasparrini A, Guo Y, Sera F, Vicedo-Cabrera AM, Huber V, Tong S, Armstrong B (2017) Projections of temperature-related excess mortality under climate change scenarios. *Lancet Planet Health* 1:e360–e367. [https://doi.org/10.1016/S2542-5196\(17\)30156-0](https://doi.org/10.1016/S2542-5196(17)30156-0)
- Giorgi F (2006) Climate change hot-spots. *Geophys Res Lett* 33(8):L08707. <https://doi.org/10.1029/2006GL025734>
- Gosling SN, Hondula DM, Bunker A, Ibarreta D, Liu J, Zhang X, Sauerborn R (2017) Adaptation to climate change: a comparative analysis of modeling methods for heat-related mortality. *Environ Health Perspect* 16(8):087008. <https://doi.org/10.1289/EHP634>
- Guilardi E, Balaji V, Callaghan S, DeLuca C, Devine G, Denvil S, Ford R, Pascoe C, Lautenschlager M, Lawrence BN (2011) The CMIP5 model and simulation documentation: a new standard for climate modelling metadata. *CLIVAR Exchanges* 56:16(2):42–46
- Guo Y, Gasparrini A, Armstrong BG, Tawatsupa B, Tobías A, Lavigne E, Sousa Zanotti Staglilio Coelho M, Pan X, Kim H, Hashizume M, Honda Y, Guo YLL, Wu CF, Zanobetti A, Schwartz JD, Bell ML, Scorticini M, Michelozzi P, Punnasiri K, Li S, Tian L, Osorio Garcia SD, Seposo X, Overcenco A, Zeka A, Goodman P, Dang TN, Van Dung D, Mayvaneh F, Nascimento Saldiva PH, Williams G, Tong S (2017) Heat wave and mortality: a multi-country, multicomunity study. *Environ Health Perspect* 125: <https://doi.org/10.1289/EHP1026>
- Healy JD (2003) Excess winter mortality in Europe: a cross-country analysis identifying key risk factors. *J Epidemiol Commun Health* 57(10):784–789. <https://doi.org/10.1136/jech.57.10.784>
- IPCC (2021) Summary for policymakers. In: Masson-Delmotte V, Zhai P, Pirani A, Connors SL, Péan C, Berger S, Caud N, Chen Y, Goldfarb L, Gomis MI, Huang M, Leitzell K, Lonnoy E, Matthews JBR, Maycock TK, Waterfield T, Yelekçi O, Yu R, Zhou B (eds) Climate change 2021: the physical science basis. contribution of working group I to the sixth assessment report of the intergovernmental panel on climate change. Cambridge University Press, Cambridge
- IPCC (2023) Climate change 2023: synthesis report. Contribution of working groups I, II and III to the Sixth assessment report of the intergovernmental panel on climate change. In: Core Writing Team, Lee H, Romero J (eds) IPCC, Geneva. <https://doi.org/10.59327/IPCC/AR6-9789291691647>
- Jacob D, Petersen J, Eggert B, Alias A, Christensen OB, Bouwer LM, Braun A, Colette A, Déqué M, Georgievski G, Georgopoulou E, Gobiet A, Menut L, Nikulin G, Haensler A, Hempelmann N, Jones C, Keuler K, Kovats S, Kröner N, Kotlarski S, Kriegsmann A, Martin E, Van Meijgaard E, Moseley C, Pfeifer S, Preuschmann S, Radermacher C, Radtke K, Rechid D, Rounsevell M, Samuelsson P, Somot S, Soussana JF, Teichmann C, Valentini R, Vautard R, Weber B, Yiou P (2014) EURO-CORDEX: new high-resolution climate change projections for European impact research. *Reg Environ Change* 14:563–578. <https://doi.org/10.1007/s10113-013-0499-2>
- Keellings D, Moradkhani H (2020) Spatiotemporal evolution of heat wave severity and coverage across the United States. *Geo Res Lett.* <https://doi.org/10.1029/2020GL087097>
- Kendall MG (1975) Rank correlation methods. Charles Griffin, London, p 120
- Kendrovski V, Baccini M, Martinez G, Wolf T, Paunovic E, Menne B (2017) Quantifying projected heat mortality impacts under 21st-Century warming conditions for selected European countries. *Int J Environ Res Public Health* 14:729. <https://doi.org/10.3390/ijerph14070729>
- Khodayar S, Paredes-Fortuny L (2024) Uneven evolution of regional European summer heatwaves under climate change. *Weather Clim Extr* 43:100648. <https://doi.org/10.1016/j.wace.2024.100648>
- King AD, Karoly DJ (2017) Climate extremes in Europe at 1.5 and 2 degrees of global warming. *Environ Res Lett* 12:114031. <https://doi.org/10.1088/1748-9326/aa8e2c>
- Kjellström E, Bärring L, Nikulin G, Nilsson C, Persson G, Strängberg G (2016) Production and use of regional climate model projections—a Swedish perspective on building climate services. *Clim Serv* 2–3:11–29. <https://doi.org/10.1016/j.ccliser.2016.06.004>
- Kodra E, Steinhaeuser K, Ganguly AR (2011) Persisting cold extremes under 21st-Century warming scenarios. *Geophys Res Lett* 38:L08705. <https://doi.org/10.1029/2011GL047103>
- Kuglitsch FG, Toreti A, Xoplaki E, Della-Marta PM, Zerefos CS, Türkes M, Luterbacher J (2010) Heat wave changes in the eastern Mediterranean since 1960. *Geophys Res Lett* 37:L04802. <https://doi.org/10.1029/2009GL041841>
- Lavaysse C, Naumann G, Alfieri L, Salamon P, Vogt J (2019) Predictability of the European heat and cold waves. *Clim Dyn* 52:2481–2495. <https://doi.org/10.1007/s00382-018-4273-5>

- Lhotka O, Kyselý J (2015) Characterising joint effects of spatial extent, temperature magnitude and duration of heat waves and cold spells over Central Europe. *Int J Climatol* 35:1232–1244. <https://doi.org/10.1002/joc.4050>
- Lionello P, Scarascia L (2018) The relation between climate change in the Mediterranean region and global warming. *Reg Environ Change* 18:1481–1493. <https://doi.org/10.1007/s10113-018-1290-1>
- Liss A, Wu R, Chui K, Naumova E (2017) Heat-related hospitalizations in older adults: an amplified effect of the first seasonal heatwave. *Sci Rep* 7:39581. <https://doi.org/10.1038/srep39581>
- Lorenzo N, Alvarez I (2022) Future changes of hot extremes in Spain: towards warmer conditions. *Nat Hazards*. <https://doi.org/10.1007/s11069-022-05306-x>
- Lorenzo N, Díaz-Poso A, Royé D (2021) Heatwave intensity of the Iberian Peninsula: future climate projections. *Atmos Res* 258:105655. <https://doi.org/10.1016/j.atmosres.2021.105655>
- Lüthi S, Fairless C, Fischer EM, Scovronick N, Armstrong B, Sousa Zanotti Staglione Coelho M, Leon Guo Y, Guo Y, Honda Y, Huber V, Kyselý J, Lavigne E, Royé D, Rytí N, Silva S, Urban A, Gasparrini A, Bresch DN, Vicedo-Cabrera A (2023) Rapid increase in the risk of heat-related mortality. *Nat Commun* 14:4894. <https://doi.org/10.1038/s41467-023-40599-x>
- Mann HB (1945) Nonparametric tests against trend. *Econometrica* 13:245–259
- Mayrhuber EAS, Dücker MLA, Wallner P, Arnberger A, Allex B, Wiesböck L, Wanka A, Kolland F, Eder R, Hutter HP, Kutalek R (2018) Vulnerability to heatwaves and implications for public health interventions—a scoping review. *Environ Res* 166:42–54. <https://doi.org/10.1016/j.envres.2018.05.021>
- MedECC (2020) Climate and environmental change in the Mediterranean Basin—current situation and risks for the future. In: Cramer W, Guiot J, Marini K (eds) First Mediterranean assessment report. Union for the Mediterranean, Plan Bleu, UNEP/MAP, Marseille, France. <https://doi.org/10.5281/zenodo.4768833>
- Merino A, Martín ML, Fernández-González S, Sánchez JL, Valero F (2018) Extreme maximum temperature events and their relationships with large-scale modes: potential hazard on the Iberian Peninsula. *Theor Appl Climatol* 133:531–550. <https://doi.org/10.1007/s00704-017-2203-9>
- Mohammed AJ, Alarcón M, Pino D (2018) Extreme temperature events on the Iberian Peninsula: statistical trajectory analysis and synoptic patterns. *Int J Climatol* 38:5305–5322. <https://doi.org/10.1002/joc.5733>
- Molina MO, Sánchez E, Gutiérrez C (2020) Future heat waves over the Mediterranean from a EURO-CORDEX regional climate model ensemble. *Sci Rep* 10:8801. <https://doi.org/10.1038/s41598-020-65663-0>
- Morais L, Lopes A, Nogueira P (2020) Which heatwave measure has higher predictive power to prevent health risks related to heat: EHf or GATO IV?—Evidence from modelling Lisbon mortality data from 1980 to 2016. *Weather Clim Extr* 30:100287. <https://doi.org/10.1016/j.wace.2020.100287>
- Moss RH, Edmonds JA, Hibbard KA, Manning MR, Rose SK, van Vuuren DP, Carter TR, Emori S, Kainuma M, Kram T, Meehl GA, Mitchell JFB, Nakicenovic N, Riahi K, Smith SJ, Stouffer RJ, Thomson AM, Weyant JP, Wilbanks TJ (2010) The next generation of scenarios for climate change research and assessment. *Nature* 463:747–756. <https://doi.org/10.1038/nature08823>
- Nairn J, Fawcett R (2013) Defining heatwaves: Heatwave defined as a heat-impact event servicing all community and business sectors in Australia. Centre for Australian Weather and Climate Research, Melbourne, p 84
- Nairn J, Fawcett R (2015) The excess heat factor: a metric for heatwave intensity and its use in classifying heatwave severity. *Int J Environ Health Res Public Health* 12:227–253. <https://doi.org/10.3390/ijerph120100227>
- Nairn J, Ostendorf B, Bi P (2018) Performance of excess heat factor severity as a global heatwave health impact index. *Int J Environ Health Res Public Health* 15(11):2494. <https://doi.org/10.3390/ijerph15112494>
- Nuñez-Hidalgo I, Meseguer-Ruiz O, Serrano-Notivoli R, Sarricolea P (2023) Population dynamics shifts by climate change: High-resolution future mid-century trends for South America. *Glob Planet Change* 226:104155. <https://doi.org/10.1016/j.gloplacha.2023.104155>
- Oliveira A, Lopes A, Soares A (2022) Excess heat factor climatology, trends and exposure across European functional urban areas. *Weather Clim Extr*. <https://doi.org/10.1016/j.wace.2022.100455>
- Ordanovich D, Tobías A, Ramiro D (2023) Temporal variation of the temperature-mortality association in Spain: a nationwide analysis. *Environ Health* 22:5. <https://doi.org/10.1186/s12940-022-00957-6>
- Paredes-Fortuny L, Khodayar S (2023) Understanding the magnification of heatwaves over Spain: Relevant changes in the most extreme events. *Weather Clim Extr* 42:100631. <https://doi.org/10.1016/j.wace.2023.100631>
- Pascaline W, Rowena H (2018) Economic losses, poverty and disaster 1998–2017. In: Report for the united nations office for disaster risk reduction, Geneva, and Center for Research on the Epidemiology of Disasters, Brussels, p 33. <https://doi.org/10.13140/RG.2.2.35610.08643>
- Pereira SC, Marta-Almeida M, Carvalho AC, Rocha A (2017) Heat wave and cold spell changes in Iberia for a future climate scenario. *Int J Climatol* 37:5192–5205. <https://doi.org/10.1002/joc.5158>
- Perkins SE (2015) A review on the scientific understanding of heat waves—their measurement, driving mechanisms, and changes at the global scale. *Atmos Res* 164–165:242–267. <https://doi.org/10.1016/j.atmosres.2015.05.014>
- Perkins SE, Alexander LV (2013) On the measurement of heat waves. *J Clim* 26:4500–4517. <https://doi.org/10.1175/JCLI-D-12-00383.1>
- Perkins-Kirkpatrick SE, Lewis SC (2020) Increasing trends in regional heatwaves. *Nat Commun* 11:3357. <https://doi.org/10.1038/s41467-020-16970-7>
- Pinto I, Rantanen M, Ødemark K, Trädowsky J, Kjellström E, Barnes C, Otto F, Heinrich D, Pereira Marghidan C, Vahlberg M, Falk K, Vautard R, Kew S, Philip S, Kimutai J, Zachariah M, Arrighi J, Forsberg A, Vaalgamaa N, Scheider L (2024) Extreme cold will still occur in Northern Europe, although less often: risking decreasing preparedness and higher vulnerability. *Grantham Inst Clim Change*. <https://doi.org/10.25561/108899>
- Piticar A, Croitoru AE, Ciupertea FA, Harpa GV (2018) Recent changes in heat waves and cold waves detected based on excess heat factor and excess cold factor in Romania. *Int J Climatol* 38:1777–1793. <https://doi.org/10.1002/joc.5295>
- Raei E, Nikoo MR, AghaKouchak A, Mazdiyasni O, Sadegh M (2018) GHWR: a multi-method global heatwave and warm-spell record and toolbox. *Sci Data* 5:180206. <https://doi.org/10.1038/sdata.2018.206>
- Ramos A, Trigo R, Santo F (2011) Evolution of extreme temperatures over Portugal: recent changes and future scenarios. *Clim Res* 48:177–192. <https://doi.org/10.3354/cr00934>
- Riahi K, Rao S, Krey V, Cho C, Chirkov V, Fischer G, Kindermann G, Nakicenovic N, Rafaj P (2011) RCP 8.5—a scenario of comparatively high greenhouse gas emissions. *Clim Change* 109:33. <https://doi.org/10.1007/s10584-011-0149-y>
- Royé D, Codesido R, Tobías A, Taracido M (2020) Heat wave intensity and daily mortality in four of the largest cities of Spain. *Environ Res* 182:09027. <https://doi.org/10.1016/j.envres.2019.109027>

- Russo S, Sillmann J, Fischer EM (2015) Top ten European heatwaves since 1950 and their occurrence in the coming decades. Environ Res Lett 10(12):124003. <https://doi.org/10.1088/1748-9326/10/12/124003>
- Sánchez-Benítez A, Barriopedro D, García-Herrera R (2020) Tracking Iberian heatwaves from a new perspective. Weather Clim Extr 28:100238. <https://doi.org/10.1016/j.wace.2019.100238>
- Scalley B, Spicer T, Jian L, Xiao J, Nairn J, Robertson A, Weeramanthri T (2015) Responding to heatwave intensity: Excess heat factor is a superior predictor of health service utilisation and a trigger for heatwave plans. Aust N Z J Public Health 39:582–587. <https://doi.org/10.1111/1753-6405.12421>
- Serrano-Notívola R, Lemus-Canovas M, Barrao S, Sarricolea P, Meseguer-Ruiz O, Tejedor E (2022) Heat and cold waves in mainland Spain: origins, characteristics, and trends. Weather Clim Extr 37(4):100471. <https://doi.org/10.1016/j.wace.2022.100471>
- Serrano-Notívola R, Tejedor E, Sarricolea P, Meseguer-Ruiz O, De Luis M, Saz MA, Longares LA, Olcina J (2023) Unprecedented warmth: a look at Spain's exceptional summer of 2022. Atmos Res 293:106931. <https://doi.org/10.1016/j.atmosres.2023.106931>
- Sheridan SC, Dixon PG, Kalkstein AJ, Allen MJ (2021) Recent trends in heat-related mortality in the United States: an update through 2018. Weather Clim Soc 13(1):95–106. <https://doi.org/10.1175/WCAS-D-20-0083.1>
- Smid M, Russo S, Costa AC, Granell C, Pebesma E (2019) Ranking European capitals by exposure to heat waves and cold waves. Urban Clim 27:388–402. <https://doi.org/10.1016/j.uclim.2018.12.010>
- Sousa PM, Barriopedro D, Ramos AM, García-Herrera R, Espírito-Santo F, Trigo RM (2019) Saharan air intrusions as a relevant mechanism for Iberian heatwaves: the record-breaking events of August 2018 and June 2019. Weather Clim Extr 26:100224. <https://doi.org/10.1016/j.wace.2019.100224>
- Spinoni J, Lakatos M, Szenthimrey T, Bihari Z, Szalai S, Vogt J, Antofie T (2015) Heat and cold waves trends in the Carpathian Region from 1961 to 2010. Int J Climatol 35:4197–4209. <https://doi.org/10.1002/joc.4279>
- Spinoni J, Vogt JV, Naumann G, Barbosa P, Dosio A (2018) Will drought events become more frequent and severe in Europe? Int J Climatol 38:1718–1736. <https://doi.org/10.1002/joc.5291>
- Strandberg G, Bärring L, Hansson U, Jansson C, Jones C, Kjellström E, Kolax M, Kupiainen M, Nikulin G, Samuelsson P, Ullerstig A, Wang S (2014) CORDEX scenarios for Europe from the Rossby Centre regional climate model RCA4. Rep Meteorol Climatol
- Taylor KE, Stauffer RJ, Meehl GA (2012) An overview of Cmip5 and the experiment design. Bull Am Meteorol Soc 93:485–498. <https://doi.org/10.1175/BAMS-D-11-00094.1>
- Tobías A, Royé D, Íñiguez C (2023a) Heat-attributable mortality in the summer of 2022 in Spain. Epidemiol 34:e5–e6. <https://doi.org/10.1097/EDE.0000000000001583>
- Tobías A, Íñiguez C, Royé D (2023b) From research to the development of an innovative application for monitoring heat-related mortality in Spain. Environ Health 1(6):416–419. <https://doi.org/10.1021/envhealth.3c00134>
- Tomczyk AM, Półrolniczak M, Kolendowicz L (2018) Cold waves in Poznań (Poland) and thermal conditions in the city during selected cold waves. Atmosphere 9:208. <https://doi.org/10.3390/atmos9060208>
- Urdiales-Flores D, Zittis G, Hadjinicolaou P, Osipov S, Klingmüller K, Mihalopoulos N, Kanakidou M, Economou T, Lelieveld J (2023) Drivers of accelerated warming in Mediterranean climate-type regions. NPJ Clim Atmos Sci 6:97. <https://doi.org/10.1038/s41612-023-00423-1>
- Van Daalen KR, Romanello M, Rocklöv J, Semenza JC, Tonne C, Markandy A, Dasandi N, Jankin S, Achebak H, Ballester J, Bechara H, Callaghan MW, Chambers J, Dasgupta S, Drummond P, Farooq Z, Gasparyan O, Gonzalez-Reviriego N, Hamilton I, Hänninen R, Kazmierczak A, Kendrovski V, Kennard H, Kiesewetter G, Lloyd SJ, Batista ML, Martinez-Urtaza J, Milà C, Minx JC, Nieuwenhuijsen M, Palamarchuk J, Quijal-Zamorano M, Robinson EJZ, Scamman D, Schmoll O, Sewe MO, Sjödin H, Sofiev M, Solaraju-Murali B, Springmann B, Triñanes J, Anto JM, Nilsson M, Lowe R (2022) The 2022 Europe report of the Lancet Countdown on health and climate change: Towards a climate-resilient future. Lancet Public Health 7:e942–e965. [https://doi.org/10.1016/S2468-2667\(22\)00197-9](https://doi.org/10.1016/S2468-2667(22)00197-9)
- Van Oldenborgh GJ, Mitchell-Larson E, Vecchi GA, de Vries H, Vautard R, Otto F (2019) Cold waves are getting milder in the northern midlatitudes. Environ Res Lett 14:114004. <https://doi.org/10.1088/1748-9326/ab4867>
- Vardoulakis S, Dear K, Hajat S, Heaviside C, Eggen B, McMichael AJ (2014) Comparative assessment of the effects of climate change on heat- and cold-related mortality in the United Kingdom and Australia. Environ Health Perspect 122(12):1285–1292. <https://doi.org/10.1289/ehp.1307524>
- Vicedo-Cabrera AM, Guo Y, Sera F, Huber V, Schleussner CF, Mitchell D, Tong S, Sousa Zanotti Staglilio Coelho M, Nascimento Saldiva PH, Lavigne E, Matus Correa P, Valdes Ortega N, Kan H, Osorio S, Kyselý J, Urban A, Jaakkola JJK, Rytí NRI, Pascal M, Goodman PG, Zeka A, Michelozzi P, Scortichini M, Hashizume M, Honda Y, Hurtado-Diaz M, Cruz J, Seposo X, Kim H, Tobias A, Íñiguez CC, Forsberg B, Oudin Åström D, Ragettli MS, Röösli M, Leon Guo Y, Wu CF, Zanobetti A, Schwartz J, Bell ML, Dang TN, Van Do D, Heaviside C, Vardoulakis S, Hajat S, Haines A, Armstrong B, Ebi KL, Gasparini A (2018) Temperature-related mortality impacts under and beyond Paris Agreement climate change scenarios. Clim Change 150:391. <https://doi.org/10.1007/s10584-018-2274-3>
- Vicedo-Cabrera AM, Scovronick N, Sera F, Royé D, Schneider R, Tobias A, Astrom C, Guo Y, Honda Y, Hondula DM, Abrutzyk R, Tong S, Souza Zanotti Staglilio Coelho M, Nascimento Saldiva PH, Lavigne E, Matus Correa P, Valdes Ortega N, Kan H, Osorio S, Kyselý J, Urban A, Orru H, Indermitte E, Jaakkola JJK, Rytí N, Pascal M, Schneider A, Katsouyanni K, Samoli E, Mayvanek F, Entezari A, Goodman P, Zeka A, Michelozzi P, Donato F, Hashizume M, Ahmad B, Hurtado Diaz M, De La Cruz VC, Overcenco A, Houthuijs D, Ameling C, Rao S, Di Ruscio F, Carrasco-Escobar G, Seposo X, Silva S, Madureira J, Holobaca IH, Fratianni S, Acquaotta F, Kim H, Lee W, Iniguez C, Forsberg B, Ragettli S, Guo YLL, Chen BY, Armstrong B, Aleman A, Zanobetti A, Schwartz J, Dang TN, Dung DV, Gillet N, Haines A, Mengel M, Huber V, Gasparini A (2021) The burden of heat-related mortality attributable to recent human-induced climate change. Nat Clim Change 11:492–500. <https://doi.org/10.1038/s41558-021-01058-x>
- Vicente C, Pereira SC, Rocha A (2019) Climate change projections of extreme temperatures for the Iberian Peninsula. Atmosphere 10(5):229. <https://doi.org/10.3390/atmos10050229>
- Vogel MM, Hauser M, Seneviratne SI (2020) Projected changes in hot, dry and wet extreme events' clusters in CMIP6 multi-model ensemble. Environ Res Lett 15:09402. <https://doi.org/10.1088/1748-9326/ab90a7>
- Wang Y, Shi L, Zanobetti A, Schwartz JD (2016) Estimating and projecting the effect of cold waves on mortality in 209 US cities. Environ Int 94:141–149. <https://doi.org/10.1016/j.envint.2016.05.008>
- Wibig J, Podstawczyńska A, Rzepa M, Piotrowski P (2009) Cold-waves in Poland—frequency, trends and relationships with atmospheric circulation. Geogr Pol 82(1):47:59. <https://doi.org/10.7163/GPol.2009.1.4>
- Wilcoxon F (1945) Individual comparisons by ranking methods. Biometrics 1:80–83

- Williams S, Venugopal K, Nitschke M, Nairn J, Fawcett R, Beattie C, Wynwood G, Bi P (2018) Regional morbidity and mortality during heatwaves in South Australia. *Int J Biometeorol* 62:1911. <https://doi.org/10.1007/s00484-018-1593-4>
- Wondmagegn BY, Xiang J, Dear K, Williams S, Hansen A, Pisaniello D, Nitschke M, Nairn J, Scalley B, Varghese BM, Xiao A, Jian L, Tong M, Bambrick H, Karon J, Bi P (2021) Impact of heatwave intensity using excess heat factor on emergency department presentations and related healthcare costs in Adelaide, South Australia. *Sci Total Environ* 781:146815. <https://doi.org/10.1016/j.scitotenv.2021.146815>
- Xu Z, FitzGerald G, Guo Y, Jalaludin B, Tong S (2016) Impact of heatwave on mortality under different heatwave definitions: a systematic review and meta-analysis. *Environ Int* 89–90:193–203. <https://doi.org/10.1016/j.envint.2016.02.007>
- Zahn M, von Storch H (2010) Decreased frequency of North Atlantic polar lows associated with future climate warming. *Nature* 467:309–312. <https://doi.org/10.1038/nature09388>
- Zittis G, Hadjinicolaou P, Klangidou M, Proestos Y, Lelieveld J (2019) A multi-model, multi-scenario, and multi-domain analysis of regional climate projections for the Mediterranean. *Reg Environ Change* 19:2621–2635. <https://doi.org/10.1007/s10113-019-01565-w>
- Zittis G, Almazroui M, Alpert P, Ciais P, Cramer W, Dahdal Y, Fnais M, Francis D, Hadjinicolaou P, Howari F, Jrrar A, Kaskaoutis DG, Kulmala M, Lazoglou G, Mihalopoulos N, Lin X, Rudich Y, Sciare J, Stenchikov G, Xoplaki E, Lelieveld J (2022) Climate change and weather extremes in the Eastern Mediterranean and Middle East. *Rev Geophys* 60:e2021RG000762. <https://doi.org/10.1029/2021RG000762>

Publisher's Note Springer Nature remains neutral with regard to jurisdictional claims in published maps and institutional affiliations.